

CrossMark  
click for updatesCite this: *RSC Adv.*, 2015, 5, 83197

# Dip in colorimetric fluoride sensing by a chemically engineered polymeric cellulose/bPEI conjugate in the solid state†

Lucio Melone,<sup>\*ab</sup> Simone Bonafede,<sup>a</sup> Dorearta Tushi,<sup>a</sup> Carlo Punta<sup>a</sup>  
and Massimo Cametti<sup>\*a</sup>Received 19th August 2015  
Accepted 24th September 2015

DOI: 10.1039/c5ra16764g

www.rsc.org/advances

The cross-linking, *via* amide bond formation, of TEMPO-oxidized cellulose nanofibers with branched-polyethyleneimine functionalized with *p*NO<sub>2</sub>-phenyl urea units generates a novel polymeric conjugate material, with a sponge-like morphology, which can be successfully used for the heterogeneous sensing of fluoride anions in DMSO solution.

## 1. Introduction

The development of materials and systems for the recognition and sensing of anionic analytes in solution is highly desirable.<sup>1–4</sup> Indeed, anionic species are commonly involved in many different biological processes related to human health and they are also key-indicators for industrial pollution or geogenic hazardous contamination.<sup>5–7</sup> Therefore, the obtainment of selective sensors for a particular anionic species could have immediate applications in fields as diverse as biochemistry, medicine and health industry, but also for environmental monitoring and land remediation. In particular, fluoride anion has become subjected to many studies. Indeed, fluoride possesses peculiar physico-chemical properties and there still exists an open debate on whether it is benign or toxic to human health at low concentration.<sup>8–10</sup> Research aimed at its recognition and sensing in solution is mainly constituted by the use of low molecular weight species, examples of which are continuously proposed in the literature.<sup>11–13</sup> Over the last recent years, polymeric systems bearing suitable sensing groups have also been considered and research in this field is growing. Indeed, polymeric systems present various unique and practical features that render them suitable for fabrication of bulk materials, more easily handled and possibly integrated in devices. Furthermore, the presence of multiple recognition sites as well as their good processability make polymeric sensors complementary to small molecule systems and, in some cases, even more appealing.<sup>14–16</sup>

As sensing often requires the use of an instrumentation which could monitor the signal produced by the sensor, the possibility of colorimetric sensing by the *naked-eye* is quite appealing for fast, qualitative and field-use applications. As far as fluoride ion sensing is concerned, the majority of polymeric systems proposed in the literature has been investigated in homogeneous solution,<sup>11,17–24</sup> while only very few examples of sensors working in heterogeneous phase are known.<sup>25–27</sup> Heterogeneous solid sensing systems may warrant an improved chemical stability and recyclability along with low sample contamination, and thus they can lead to important developments in the construction of devices of practical use, especially if coupled with *naked-eye* recognition ability.

Among the possible materials useful for the development of heterogeneous sensors, cellulose could play an important role. Cellulose is an abundant and renewable biopolymer, with good mechanical properties and it can be chemically functionalized in order to modify its physical and chemical behavior. In particular, nanostructured cellulose, such as cellulose nanocrystals, cellulose nanowhiskers, micro-/nanofibrillated cellulose, and cellulose nanofibers (CNF), has become a promising building block for the preparation of innovative functional materials useful in a wide number of applications.<sup>28–35</sup> Furthermore, due to their morphology, low density, high specific strength and modulus, high surface area and the presence of surface –OH groups, CNF can form highly porous aerogels having intriguing properties.<sup>36–39</sup>

Recently, our group showed that TEMPO-oxidized cellulose nanofibers (TOCNF) can be used for the preparation of water-stable sponge-like materials useful for water remediation by the direct amidation of the TOCNF carboxylic groups with branched-polyethyleneimine (bPEI), without using a supplementary cross-linker.<sup>40</sup>

The TOCNF-bPEI sponges showed high adsorption capability towards both organic and heavy metals pollutants. The preparative protocol relied on the freeze-drying of aqueous

<sup>a</sup>Department of Chemistry, Materials and Chemical Engineering “G. Natta”, Politecnico di Milano, Piazza L. Da Vinci 32, 20133 Milano, Italy. E-mail: lucio.melone@polimi.it; massimo.cametti@polimi.it

<sup>b</sup>Università Telematica e-Campus, Via Isimbardi 10, 22060 Novedrate, Como, Italy

† Electronic supplementary information (ESI) available. See DOI: 10.1039/c5ra16764g

**TOCNF-bPEI** dispersions followed by the thermal treatment. Based on the interesting results obtained so far, we envisaged that an analogous synthetic approach could be extended for the engineering of porous solids for the heterogeneous sensing of fluoride ion.

Among the different sensing units, the urea moiety can be considered quite appealing, as demonstrated by the works by Fabbri et al. where the properties of urea derivatives, in terms of their response to anionic analytes, have been investigated.<sup>41–44</sup> In polar aprotic solvents, urea derivatives substituted with electron withdrawing groups can undergo deprotonation in the presence of relatively basic anion and this results in conspicuous color changes.<sup>44</sup> Examples of polymeric materials embedded with urea groups and used as homogeneous sensors for anions in solution have recently been described.<sup>45–51</sup>

Here, we report on the synthesis, characterization and anion responsiveness of a novel polymeric material obtained from **TOCNF** cross-linked with **bPEI** functionalized with *p*NO<sub>2</sub>-phenyl urea moieties (named **TOCNF-bPEI-Sens** hereafter). The role of such strong electron withdrawing moiety is twofold. On one hand, it renders the amidic NH more acidic and more prone to interact with the anionic species, while, on the other, it enables the colorimetric response upon NH's deprotonation. At variance with the majority of polymeric anion sensors reported to date, which work in solution of weakly polar solvents (THF, CHCl<sub>3</sub>, CH<sub>2</sub>Cl<sub>2</sub>, etc.), this material was purposely optimized so that it could change its color – from yellow to vivid orange/red – when dipped in a DMSO solution containing fluoride anion, while maintaining its solid state. Notably, this response is clearly visible by the *naked-eye* and it is selective for fluoride over chloride, and more importantly, over other commonly competing anions such as acetate (AcO<sup>−</sup>) and dihydrogenphosphate (H<sub>2</sub>PO<sub>4</sub><sup>−</sup>).<sup>11–13</sup> To the best of our knowledge, no attempts towards the development of solid sensors for anions using cellulose, or other biopolymers, as scaffold have been yet reported.

## 2. Experimental

### 2.1. Materials

**bPEI** (25 kDa) was purchased from Sigma-Aldrich. The content of primary amino groups was determined from a <sup>13</sup>C NMR spectrum of **bPEI** in D<sub>2</sub>O (≈ 100 mg mL<sup>−1</sup>, 10 000 scans, probe temperature 30 °C) using inverse gated decoupling sequences to avoid NOE effects, according to the paper of von Harpe et al.<sup>52</sup> A value of 7.43 mmol g<sup>−1</sup> of primary NH<sub>2</sub> groups was obtained. Further details on the calculations are reported in a recently published work.<sup>40</sup> A 2% w/v solution of **bPEI** in THF (400 mL) was prepared and dried onto CaH<sub>2</sub> until no further H<sub>2</sub> formation was observed (about 48 h). For the preparation of **bPEI-Sens** (*n*%) (with *n* = 2, 5, 10), 100 mL of the previous solution were introduced into a 250 mL two-necked round bottom flask, diluted with 100 mL of anhydrous THF and kept in ice bath, under slow flow of nitrogen. The required amount of 4-nitrophenyl isocyanate (297.2 mg for **bPEI-Sens**(2%), 743 mg for **bPEI-Sens** (5%), 1486 mg for **bPEI-Sens** (10%)) was dissolved into 20 mL of anhydrous THF and added drop-wise with a

dropping funnel in 1 h. The reaction mixture was kept under stirring at 0 °C for 6 h and then at room temperature overnight. The solvent was finally evaporated under vacuum. The product was dissolved into 5 mL of HCl 0.5 M and purified by dialysis (cut-off: ≈ 12.4 kDa) for 24 h against HCl 0.1 M and for 24 h against NH<sub>4</sub>OH 0.1 M. Finally, water was removed with a rotary evaporator obtaining a sticky yellow solid that was kept under vacuum (<5 mbar) for 6 h at 40 °C.

Cotton cellulose was oxidized as detailed in the ESI† in order to obtain **TOCNF** with two different amounts of COOH groups (**TOCNF1**, 0.83 mmol g<sup>−1</sup>; **TOCNF2**, 1.54 mmol g<sup>−1</sup>). **TOCNF-bPEI-Sens** specimens were prepared with a procedure similar to the one described in the ref. 40. Specifically, aqueous dispersions of **TOCNF1** or **TOCNF2** (3.5% w/v of dry **TOCNF**) containing **bPEI-Sens** (*n*%) (with **bPEI-Sens** : **TOCNF** = 2 : 1, w/w) were introduced into a 96-well-plate, frozen at −80 °C for 24 h and finally freeze-dried at −60 °C for 48 h obtaining pale yellow cylindrical sponges. The solid material was thermally treated in oven, increasing the temperature stepwise from 60 °C to 102 °C over 8 h, and then keeping the temperature at 102 °C for 2 additional hours. The samples were washed with DMSO (50 mL at 50 °C for 1 h, 5 times), HCl 0.1 M (50 mL at r.t. for 1 h, 3 times), NH<sub>4</sub>OH 0.1 M (50 mL at r.t. for 1 h, 3 times), and acetone (50 mL at r.t. for 1 h, 3 times), finally dried in air at r.t. for 48 h and in oven (70 °C) for 2 h.

The model derivative **1** was synthesized from propargylamine and *p*NO<sub>2</sub>-phenyl isocyanate following a published procedure.<sup>47</sup> Additional characterization can be found in the ESI.†

### 2.2. Characterization

The solid phase FT-IR spectra of the powdered sample with infrared grade KBr were obtained using a Varian 640-IR spectrometer. <sup>1</sup>H-NMR spectra were acquired with a Bruker Avance 500 MHz. The <sup>13</sup>C cross polarization magic angle spinning (CP-MAS) spectra were recorded with an FT-NMR Avance™ 500 (Bruker BioSpin S.r.l), with a superconducting ultrashield magnet of 11.7 tesla operating at 125.76 MHz <sup>13</sup>C frequency. The following conditions were applied: repetition time 4 s, <sup>1</sup>H 90 pulse length 4.0 μs, contact time 1.2 ms and spin rate 8 kHz. The compounds were placed in a zirconium rotor, 4 mm in diameter and 18 mm high. The chemical shifts were recorded relative to glycine standard, previously acquired (C=O signal: 176.03 ppm, relative to tetramethylsilane reference). Scanning electron microscopy (SEM) was performed using a variable pressure instrument (SEM Cambridge Stereoscan 360) at 100/120 Pa with a detector VPSE. The operating voltage was 20 kV with an electron beam current intensity of 150 pA. The focal distance was 8 mm. The specimens were used without any treatment. UV-vis measurements in solution were recorded on a Perkin Helmer 835 spectrophotometer thermostated at 25 °C. Spectral data were then analysed with SigmaPlot 11.0. UV-vis solid state spectra were recorded by a Jasco 60 mm integrating sphere working in the range of 300–600 nm (UV-vis band width: 2.0 nm; scan: 100 nm min<sup>−1</sup>; data pitch 0.5 nm). The spectra were analyzed using the instrument software package



converting the diffuse reflectance data in absorbance-like data by the Kubelka–Munk equation.

### 3. Results and discussion

Natural cellulose provides an excellent scaffold for the development of engineered functional materials. The synthetic strategy chosen to produce the desired **TOCNF-bPEI-Sens** material is schematically depicted in Scheme 1. At first, natural cotton cellulose and **bPEI** were separately functionalized with carboxylic groups and urea moieties, respectively, and then the two polymers were mixed and cross-linked together by thermal amidic bond formation. Cellulose was oxidized to **TOCNF** by a well-established NaClO/TEMPO method.<sup>53,54</sup> This approach leads to the oxidation of the primary hydroxyl groups of the anhydroglucose units mainly forming the corresponding carboxylic acids.<sup>53</sup> The quantification of the oxidation degree was obtained by acid–base titration and, as expected, the number of moles of COOH groups per gram of cellulose increased along with the amount of NaClO employed (see ESI† for further details). **TOCNF** with two different contents of carboxylic acid units, namely **TOCNF1** (0.83 mmol g<sup>−1</sup>) and **TOCNF2** (1.54 mmol g<sup>−1</sup>), were used for the preparation of the **TOCNF-bPEI-Sens** sponges. The degree of oxidation of the cellulose is one of the parameters that could introduce tunability in the material design, and we were interested to verify whether this aspect could affect the sponges' colorimetric response in presence of fluoride ions.

**bPEI** is a commercially available polymer. Due to its branched structure and the presence of amino groups (primary, secondary and tertiary), **bPEI** in water is a polycationic macromolecule with high ionic charge density, widely used as gene therapy delivery agent.<sup>55</sup>

Three kinds of **bPEI-Sens** derivatives with increasing contents of *p*NO<sub>2</sub>-phenyl urea units were prepared by changing

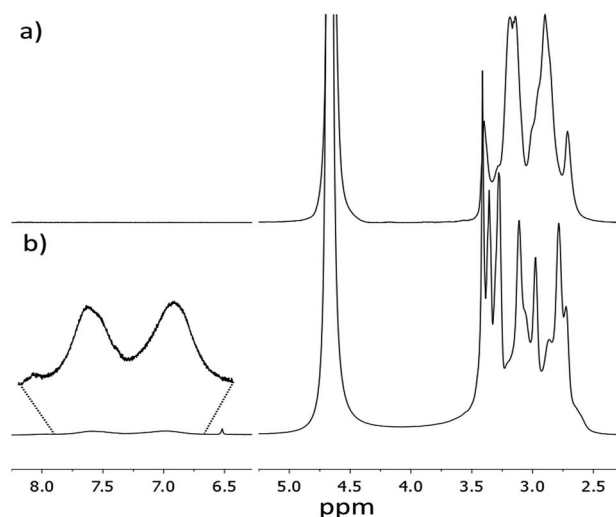
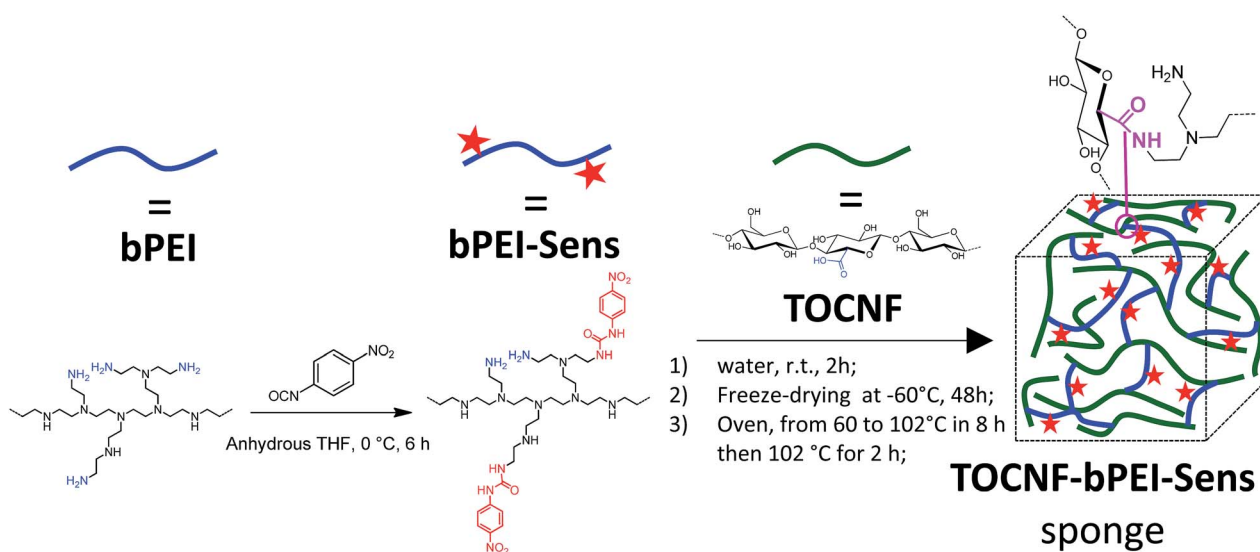


Fig. 1 <sup>1</sup>H-NMR spectra of: (a) **bPEI**; (b) **bPEI-Sens** (10%). Solvent: D<sub>2</sub>O + CF<sub>3</sub>COOH, *T* = 23 °C.

the amount of the *p*NO<sub>2</sub>-phenyl isocyanate with respect to the content of primary amino groups of **bPEI** (7.43 mmol g<sup>−1</sup>).

Hereafter, these derivatives are labelled as **bPEI-Sens** (*n*%), where *n*% is the nominal molar percentage of *p*NO<sub>2</sub>-phenyl isocyanate used with respect to the –NH<sub>2</sub> groups (*n* = 2, 5, 10). Fig. 1 shows the <sup>1</sup>H-NMR spectra of the pristine **bPEI** (a) and the **bPEI-Sens** (10%) in D<sub>2</sub>O acidified with few drops of CF<sub>3</sub>COOH (b). The set of peaks in the range 2.5–4.0 ppm is attributed to the –CH<sub>2</sub>–CH<sub>2</sub>– protons. The aromatic protons of the *p*NO<sub>2</sub>-phenyl urea moieties are visible as two broad peaks in the range 6.7–7.9 ppm (Fig. 1b, inset). Due to the broadness and the intrinsic low intensity of these signals, we chose not to rely on the NMR data above for the precise evaluation of the actual degree of functionalization (*vide infra*). **bPEI-Sens** (*n*%) specimens with *n* > 10 (for example *n* = 20) were also synthesized. Unfortunately, they



Scheme 1 Synthetic procedure for the preparation of **TOCNF-bPEI-Sens** sponges.



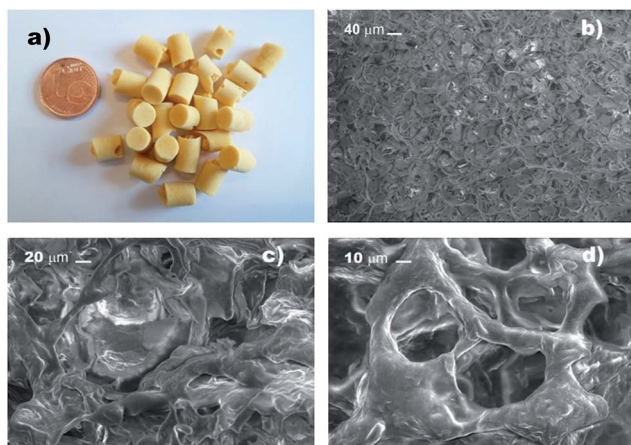


Fig. 2 (a) TOCNF-bPEI-Sens sponges; (b–d) SEM images at different magnification.

were not sufficiently soluble in water as requested for the preparation of the **TOCNF-bPEI-Sens** sponges. Following the procedure reported in Scheme 1, cylindrical shaped **TOCNF-bPEI-Sens** specimens were obtained (Fig. 2a). They were mechanically stable in water both at acidic pH ( $\sim 1$ ) and basic pH ( $\sim 13$ ), in DMSO and in other common organic solvents. SEM analysis showed a porous structure with pore size ranging from few to hundred micrometers and thin pore walls (Fig. 2b–d). The FT-IR spectra of **TOCNF1-bPEI-Sens** (10%) and **TOCNF2-bPEI-Sens** (10%) are reported in Fig. 3a and b, respectively. The peak associated to the stretching vibration of the amidic C=O bond is found at  $1666\text{ cm}^{-1}$ . A difference in the intensity of this peak between the two specimens can be observed. This can be attributed to the different oxidation degree of the starting **TOCNF**. The band associated to the amine N–H stretching is located around  $3300\text{ cm}^{-1}$ , partially overlapping with the broad O–H stretching band found between  $3000\text{ cm}^{-1}$  and  $3700\text{ cm}^{-1}$ . The peaks in the  $2800\text{--}3000\text{ cm}^{-1}$  range are attributed to the

C–H stretching vibration modes of cellulose and **bPEI**, overlapping in this region. The  $^{13}\text{C}$  CP-MAS spectrum of **TOCNF2-bPEI-Sens** (10%) is reported in Fig. 3c. The characteristic peaks of the carbons of the anhydroglucose units can be clearly seen in the  $60\text{--}120\text{ ppm}$  range. Their assignment can be found in the literature.<sup>56</sup> The residual carboxylic carbons (as  $\text{COO}^-$ ) not involved in the amide bond formation with **bPEI-Sens** give a signal located at  $174\text{ ppm}$ , while the amidic carbons signal is located upfield at  $164\text{ ppm}$ .<sup>40</sup> Finally, the broad signal at  $35\text{--}60\text{ ppm}$  is ascribed to the  $\text{CH}_2$  carbons of the grafted **bPEI**. In both FT-IR and  $^{13}\text{C}$  CP-MAS spectra, it was not possible to detect the signals associated to the sensing units, most probably due to the low functionalization degree of **bPEI** with the  $p\text{NO}_2$ -phenyl urea moieties.

In order to evaluate the UV-vis response of the new material **TOCNF-bPEI-Sens** to the presence of common anions, added as their tetrabutyl ammonium (TBA) salts, we first investigated the solution behavior of the model compound **1** (Table 1), and of the functionalized **bPEI-Sens** (10%). As to the model compound, we expected it to display the typical behavior of urea derivatives decorated with strong electron withdrawing groups. Fig. 4a shows the family of spectra obtained by the addition of (TBA) AcO to a solution of **1** in DMSO at  $25^\circ\text{C}$ . A bathochromic shift of *ca.*  $20\text{ nm}$  is observed for the only unstructured absorption band of **1**, along with the appearance of an isosbestic point at  $351\text{ nm}$  which is consistent with the formation of a hydrogen bond (HB) complex between **1** and the acetate anion (Scheme 2a). The dataset shown in Fig. 4b, *i.e.*, the absorbance at  $367\text{ nm}$  ( $A_{367}$ ) plotted against the concentration of acetate anion ( $[\text{AcO}^-]$ ) can be fitted with a standard non-linear least square procedure, considering a  $1:1$  binding isotherm. Similar absorption changes can be observed upon addition of (TBA)Cl and (TBA)  $\text{H}_2\text{PO}_4$  salts to **1** (see ESI†). Table 1 summarizes the association constants  $K\text{ (M}^{-1}\text{)}$  and the variation of the extinction coefficient at the chosen wavelength ( $\Delta\epsilon_{\text{max}}$ ) as obtained by the titration experiments. As expected, acetate and phosphate bind well to **1**, with an association constant slightly higher for acetate.

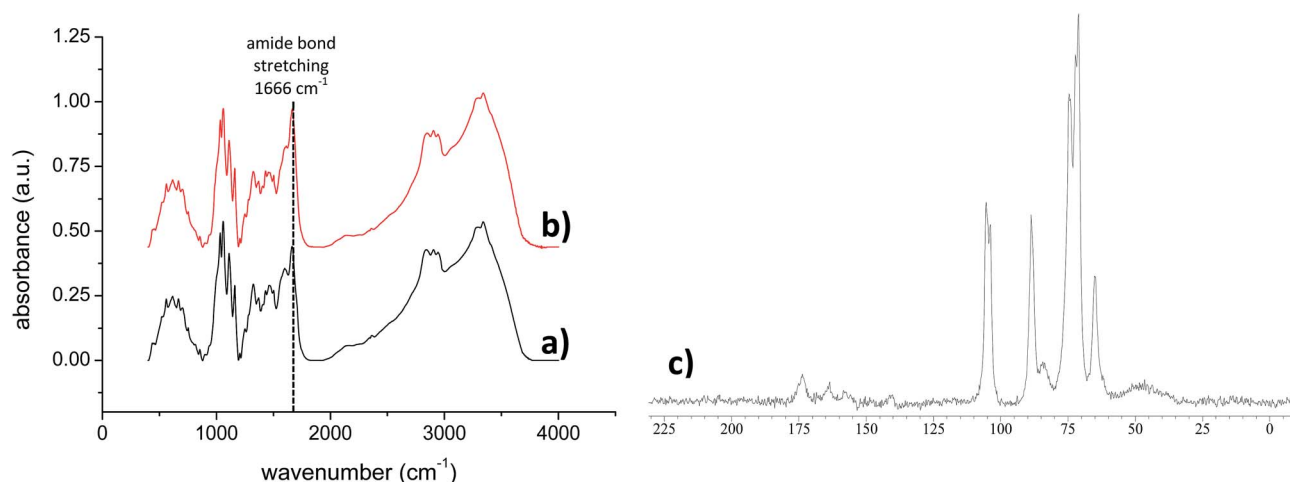


Fig. 3 FT-IR spectra (KBr) of (a) **TOCNF1-bPEI-Sens** (10%) and (b) **TOCNF2-bPEI-Sens** (10%);  $^{13}\text{C}$  CP-MAS solid state NMR spectrum of **TOCNF2-bPEI-Sens** (10%) (c).





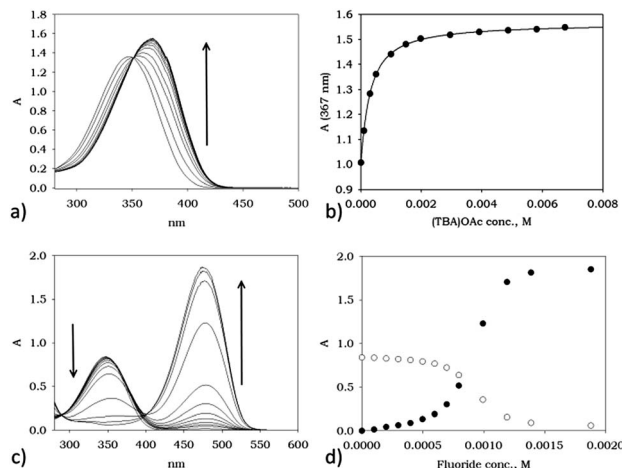
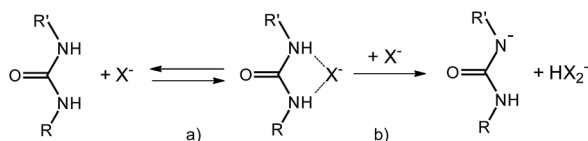


Fig. 4 (a) Family of spectra obtained upon addition of increasing amount of (TBA)OAc to a  $9.1 \times 10^{-5}$  M solution of **1**; (b) Abs vs. AcO concentration titration plot at 367 nm, line corresponds to the calculated fit of the experimental data points, see Table 1; (c) family of spectra obtained upon addition of increasing amount of (TBA)F to a  $5.4 \times 10^{-5}$  M solution of **1**; (d) Abs vs.  $F^-$  concentration titration plots at 350 nm (○) and 476 nm (●); all measurements were made at 298 K in DMSO.

Chloride, instead, is bound to **1** several tenths of times less efficiently. Different is the behavior of fluoride. As seen in Fig. 4c, addition of this ion to **1**, under the same experimental conditions, induces the formation of a completely new and intense band whose absorption maximum is at 476 nm. Such drastic changes are on account of the deprotonation of one of the urea amidic NH groups. Titration plots at 350 and 476 nm are shown in Fig. 4d, and they confirm by the classic sigmoid shape the peculiar characteristic of fluoride anion which is able to act as a relatively strong base in polar aprotic solvent due to the formation of the stable bifluoride  $HF_2^-$  ion. A slight deviation from an ideal single process mode is actually hinted by the presence of two concentration dependent isosbestic points. The first, at 375 nm is present at low  $F^-$  concentration regime and it is due to an initial HB adduct formation which, as the  $F^-$  concentration increases, is eventually driven towards deprotonation (Scheme 2a and 2b). As already noted by others,<sup>41–43</sup> the deprotonation of this type of urea derivatives causes intense changes in the absorption spectra and that results in the appearance of intense color, visible to the naked-eye. The striking difference in the anion response of **1** is at the basis of development of a selective chromogenic sensor for fluoride anion. Although all functionalized **bPEI-Sens** (*n*%) derivatives



Scheme 2 Schematic view of the HB complex formation (a), and of the deprotonation step occurring when  $X = F$ , (b).

Table 1 Association constants ( $K$ ,  $M^{-1}$ ) for HB complexes between compound **1** and selected anions in DMSO- $d_6$  at 300 K

Anion	$K (\pm \sigma)$	$\Delta \epsilon$ (nm)
Chloride	$50 \pm 20$	500 (349)
Phosphate	$2400 \pm 70$	5600 (367)
Acetate	$3870 \pm 70$	6150 (367)
Fluoride <sup>a</sup>	—	—

<sup>a</sup> The initial association step (Scheme 2) cannot be adequately monitored due the occurrence of a subsequent deprotonation.

were expected to behave similarly to **1**, **bPEI-Sens** (10%) was tested in DMSO solution nonetheless.

Indeed, polymeric **bPEI-Sens** (10%) responds to the presence of anions in a way which is qualitatively similar to the model compound **1**. More detailed, acetate anions induce a bathochromic shift of *ca.* 15 nm of the absorption band as shown in Fig. 5a and an isosbestic point is clearly visible at 353 nm. Addition of phosphate anion leads to similar UV-vis changes (see ESI†). Hill plots (Fig. 5b) indicated a slightly anti-cooperative behavior ( $m = 0.71$  and  $0.64 < 1$  for acetate and phosphate, respectively – see ESI† for further information),

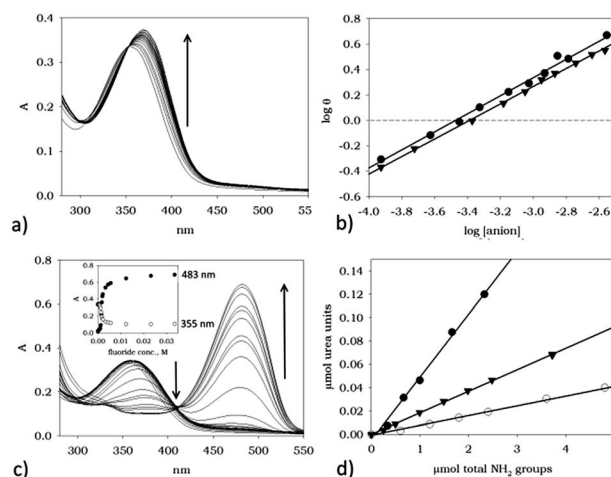


Fig. 5 (a) Family of spectra obtained upon addition of increasing amount of (TBA)OAc to a  $0.3 \text{ mg mL}^{-1}$  solution of **bPEI-Sens** (10%); (b) Hill plots relative to the association of  $AcO^-$  (●) and  $H_2PO_4^-$  (▼) ions to **bPEI-Sens** (10%); (c) family of spectra obtained upon addition of increasing amount of (TBA)F to a  $0.3 \text{ mg mL}^{-1}$  solution of **bPEI-Sens** (10%), inset: plot of the changes in Abs upon addition of  $F^-$  at selected wavelengths; (d) plots of  $\mu\text{mol}$  of  $pNO_2$ -phenyl urea group vs.  $\mu\text{mol}$  of total  $NH_2$  for the **bPEI-Sens** (*n*%) *n* = 2% (○), 5% (▼) and 10% (●); all measurements were carried out at 298 K in DMSO.

while the averaged microscopic association constants,  $K$ , are similar to those found with the model compound **1** ( $\log K = 3.6$  and  $3.5$  for phosphate and acetate, respectively).<sup>57</sup> As to chloride anion, the decrease in binding efficiency with respect to  $\text{AcO}^-$  and  $\text{H}_2\text{PO}_4^-$ , as already seen with **1**, is also displayed by the polymeric material **bPEI-Sens** (10%) whose absorption spectrum is not significantly affected by increasing the chloride concentration (up to  $0.015\text{ M}$ ). This led us to consider its binding as negligible under these experimental conditions ( $\text{ESI}^\dagger$ ). Fluoride, instead, induces more drastic changes in the absorption spectrum of **bPEI-Sens** (10%) (Fig. 5c). A new band, centered at  $476\text{ nm}$ , appears upon addition of  $\text{F}^-$ . A slightly sigmoidal titration profile is also observed (Fig. 5c, inset).

Additional UV-vis investigation can also provide a quantitative check of the actual degree of functionalization of the **bPEI** derivatives. Considering that the absorption of **bPEI** derivatives is negligible at  $476\text{ nm}$  (where the new band appears) and by assuming the average molar extinction coefficient of the  $p\text{NO}_2$ -phenyl urea groups and that of **1** to be equal,  $A_{476}$  can be taken as being proportional to the concentration of the  $p\text{NO}_2$ -phenyl urea groups present on the polymer. A weighted sample of each **bPEI-Sens** ( $n\%$ ) is introduced in a vessel containing  $1\text{ mL}$  of DMSO and an excess of (TBA)F. Known aliquots of dissolved polymer are then added to a DMSO solution in a cuvette and the absorption spectra are recorded. Plots of  $\mu\text{mol}$  of urea units vs.  $\mu\text{mol}$  of available  $\text{NH}_2$  groups are shown in Fig. 5d. The observed slopes correspond to  $0.9\%$ ,  $2.0\%$  and  $6.1\%$  of actual functionalization for the **bPEI-Sens** ( $n\%$ ) with  $n = 2, 5$  and  $10$ , respectively (see  $\text{ESI}^\dagger$ ). These figures, thus, corresponds to the actual percentage of primary amines reacted with  $p\text{NO}_2$ -phenyl isocyanate and approximately to half of the nominal functionalization value (see Experimental part). The calculation obviously rests on the assumption that a complete deprotonation of all the urea groups takes place under the condition of large excess of fluoride anion employed. This assumption is clearly more valid the least the percentage of functionalization of **bPEI** derivatives is.

Again, the polymeric material **bPEI-Sens** (10%) responds to the presence of fluoride in a way that enables its selective sensing, since the presence of other common anions, such as chloride, acetate and phosphate, do not induce changes in their absorption spectra, nor a colorimetric response as conspicuous as for  $\text{F}^-$ . We thus envisaged that, if such anion responsiveness were implemented into a solid material, a solid state sensor for fluoride anion could indeed be achievable. An optimal practical test for the detection of anionic analytes in solution requires a material which is stable, easily handled and which does not necessitate particular attention for its storage. Furthermore, it should allow for multiple uses and, most importantly, be able to provide a *naked-eye* sensing, thus avoiding the use of any instrumentation. A disk of **TOCNF2-bPEI-Sens** (10%) maintains its original yellow color and solidity, consistency, and texture, when immersed in DMSO (Fig. 6a), while when dipped into a  $0.05\text{ M}$  solution of (TBA)F, its color changes to a light orange (Fig. 6b). More striking is the color variation at higher concentration of fluoride ( $0.5\text{ M}$ ). In this case (Fig. 6c), the **TOCNF2-bPEI-Sens** (10%) acquires a deep orange/red hue.<sup>58</sup> Such change

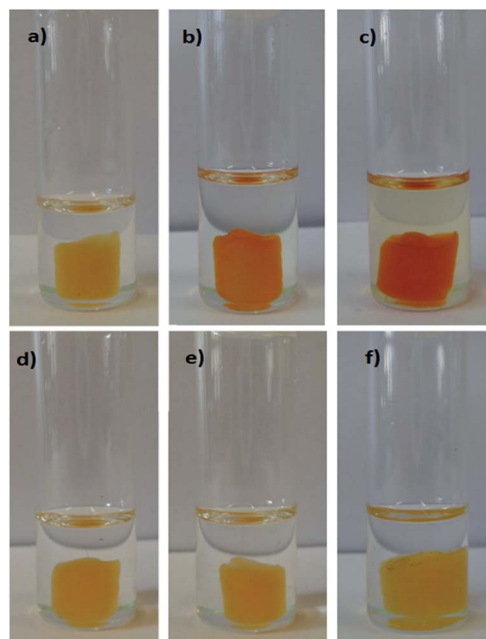


Fig. 6 TOCNF2-**bPEI-Sens** (10%) in DMSO (a), (TBA)F  $0.05\text{ M}$  (b), (TBA)F  $0.5\text{ M}$  (c), (TBA)Cl  $0.5\text{ M}$  (d), (TBA)AcO  $0.5\text{ M}$  (e), (TBA) $\text{H}_2\text{PO}_4$   $0.5\text{ M}$  (f). Temperature:  $55^\circ\text{C}$ . Contact time:  $30\text{ min}$ .

allows for a direct visual detection of fluoride (compare Fig. 6a to c). Notably, this material is quite selective a sensor. Indeed, no common interfering anions, such as acetate and phosphate, nor chloride, do lead to any color change under such experimental conditions (Fig. 6d–f).

Contrary to our original expectations, in presence of (TBA)F  $0.5\text{ M}$ , no evident colorimetric differences between **TOCNF1-bPEI-Sens** (10%) and **TOCNF2-bPEI-Sens** (10%) could be detected by the *naked-eye* (Fig. S13 $^\dagger$ ). This indicates that the degree of oxidation of the cellulose used for the preparation of the materials, at least considering the values adopted in this work, cannot be considered as an effective parameter for the modulation of the colorimetric response of the sensor material. Differently, the degree of functionalization of the **bPEI** shows more marked effect. Indeed, in presence of (TBA)F  $0.5\text{ M}$ , the color change of the samples obtained from **TOCNF2** with **bPEI** at different nominal contents of  $p\text{NO}_2$ -phenyl urea groups (from  $2\%$  to  $10\%$ ) gradually increases from the original yellow to pale orange and to bright orange (Fig. S14 $^\dagger$ ).

The above mentioned visual response of the **TOCNF-bPEI-Sens** sponges to fluoride ions was additionally characterized by solid state UV-vis spectroscopy. Fig. 7 shows the absorption spectrum of **TOCNF2-bPEI-Sens** (10%) as obtained at the end of the synthetic procedure (inset) and after the immersion in a  $0.5\text{ M}$  solution of (TBA)F in DMSO once the excess solvent was removed. Although quite broad, the two bands are prominently different and the increase in absorption at higher wavelength is evident. These data give an instrumental characterization of the *naked-eye* color change observed in the material and are in line with the measurements obtained in solution for **1** and



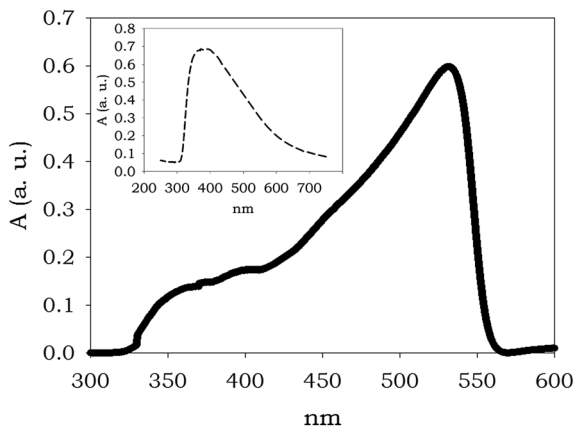


Fig. 7 Reflectance spectrum of TOCNF2-bPEI-Sens (10%) after immersion into a solution of (TBA)F 0.5 M,  $A_{\max} = 532$  nm; the spectrum of DMSO-wet TOCNF2-bPEI-Sens (10%) was taken as baseline; inset: spectrum of the TOCNF2-bPEI-Sens (10%),  $A_{\max} = 392$  nm.

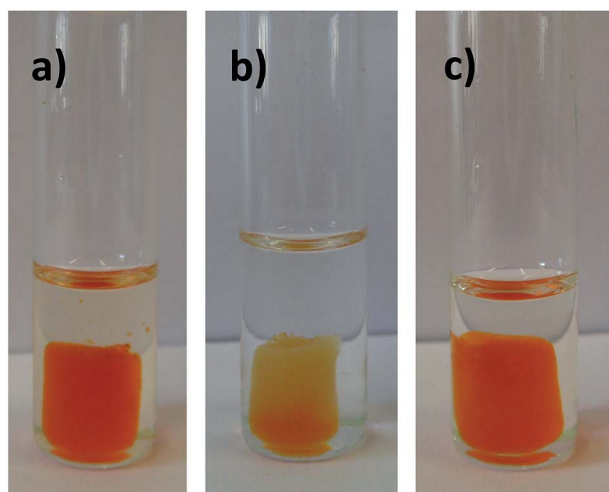


Fig. 8 TOCNF2-bPEI-Sens (10%) in TBAF 0.5 M (DMSO) (a), during its regeneration in MeOH (b) and final reuse in TBAF 0.5 M (DMSO) (c). Temperature: 55 °C. Contact time: 30 min.

**bPEI-Sens** (10%). A similar behavior was observed for all the other derivatives.

As said, re-usability of a functional material is a quite important property, which is related both to practicalness and to the economic viability of its eventual utilization in real-world applications. The presented materials have indeed proven to be re-usable, as demonstrated by the experiment visualized in Fig. 8. Once the **TOCNF2-bPEI-Sens** (10%) sponge has detected fluoride in DMSO solution by turning reddish (Fig. 8a), it can be re-generated by immersion in MeOH. This treatment quickly reinstates the original yellow color of the sponge (Fig. 8b shows this process), and ensures several reiterations of the fluoride responsive process (Fig. 8c), after methanol solvent evaporation.

Finally, we would like to add a note concerning the role of the solvent in this process. As said, the **TOCNF-bPEI-Sens**

materials were tested in DMSO, a strongly polar and competitive solvent. Anhydrous solvent is, however, mandatory if a marked response is sought, since the presence of water, or any protic solvent, is highly detrimental to the development of color. This did not come as a surprise, given that a deprotonation process is at the basis of the selective sensing event and the use of methanol for the material regeneration is in line with these observations. Anyway, one might suggest that the use of a solvent of lower polarity such as  $\text{CHCl}_3$  would increase the response of the material. Arguably, this is not the case for the present system and, in fact, dipping **TOCNF-bPEI-Sens** (10%) into a 0.5 M solution of fluoride in chloroform does not produce any noticeable effect. Such seemingly counter-intuitive result is probably due to unfavorable solvation effects, as charges can be more poorly solvated in chloroform than in DMSO, especially on a polymeric material where charge accretion can occur.

## 4. Conclusions

We have presented the fabrication, the characterization and the study on the sensor capability of a novel functional material based on the cross-linking between TEMPO-oxidized cellulose and **bPEI** decorated with *p* $\text{NO}_2$ -phenyl urea groups. This material, **TOCNF-bPEI-Sens**, is capable to recognize fluoride anion by a color change, visible by the *naked-eye*, when dipped into a DMSO solution containing the anion. Also, we have demonstrated that such response is selective for fluoride over commonly competing anions such as acetate and phosphate. The proposed sensor is solid and remains as such during the sensing process which, therefore, occurs in a heterogeneous system. On this regards, this work represents a novelty since the vast majority of polymeric sensors reported to date operate in homogeneous phase. Moreover, this work presents a smart and innovative way to use CNF for sensing applications. A detailed UV-vis study on a model compound, **1**, on intermediate **bPEI-Sens** (10%) in solution and on **TOCNF2-bPEI-Sens** (10%) directly in the solid state, confirms the nature of the chemical process responsible for the color change, as being due to deprotonation of the urea moiety. This feature allows for a complete reusability of the sensor, which can be regenerated by washing with methanol.

It is important to highlight here that the absence of colorimetric response with the **TOCNF-bPEI-Sens** materials in aqueous environments is intrinsically related to the specific sensing unit adopted in this work and not to the methodological approach followed for the preparation of the materials. Recently, different compounds have been proposed for the sensing of fluoride ions directly in water.<sup>59–61</sup> Considering the simplicity of the synthetic protocol for the preparation of **TOCNF-bPEI-Sens** materials, we envisage that the functionalization of **bPEI** with similar sensing units followed by its cross-linking with **TOCNF** could indeed represent a valid methodology for the preparation of solid state sensors for the detection of  $\text{F}^-$  ions in protic solvents and, eventually, in water.



## Acknowledgements

The authors gratefully acknowledge Prof. E. Vismara for the access to the integrating sphere equipment used in the solid state UV-vis measurements. M. C. thanks the Programma per Giovani Ricercatori "Rita Levi Montalcini" – 2009; The Ministry for Education, University and Research (MIUR) is kindly acknowledged through the Research Project PRIN-2010-2011-PROxi project 2010PFLRJR\_005.

## Notes and references

- 1 Recognition of Anions, in *Top. Curr. Chem.*, ed. R. Vila, Springer, 2008, vol. 129.
- 2 *Top. Curr. Chem.*, ed. I. Stibor, 2005, vol. 255.
- 3 *Chemosensor. Principles, Strategies, and Applications*, ed. B. Wang and E. V. Anslyn, John Wiley & Sons, Inc., Hoboken, New Jersey, 2011.
- 4 Anion Recognition in Supramolecular Chemistry, in *Top. Heterocyclic Chem.*, ed. P. A. Gale and W. Dehaen, vol. 24, SpringerCity, 2010.
- 5 A. Bhatnagar and M. Sillanpää, *Chem. Eng. J.*, 2011, **168**, 493–504.
- 6 A. Bhatnagar, E. Kumar and M. Sillanpää, *Chem. Eng. J.*, 2011, **171**, 811–840.
- 7 C. Warwick, A. Guerreiro and A. Soares, *Biosens. Bioelectron.*, 2013, **41**, 1–11.
- 8 S. Peckham, *Crit. Publ. Health*, 2012, **22**, 159–177.
- 9 J. Aaseth, M. Shimshi, J. L. Gabrilove and G. S. Birketvedt, *J. Trace Elem. Exp. Med.*, 2004, **17**, 83–92.
- 10 R. A. Freeze and J. H. Lehr, in *The Fluoride Wars: How a Modest Public Health Measure Became America's Longest-Running Political Melodrama*, Wiley, Hoboken, NJ, 2009.
- 11 Y. Zhou, J. F. Zhang and J. Yoon, *Chem. Rev.*, 2014, **114**, 5511–5571.
- 12 M. Cametti and K. Rissanen, *Chem. Soc. Rev.*, 2013, **42**, 2016–2038.
- 13 M. Cametti and K. Rissanen, *Chem. Commun.*, 2009, 2809–2829.
- 14 A. Rostami and M. S. Taylor, *Macromol. Rapid Commun.*, 2012, **33**, 21–34.
- 15 J. M. García, F. C. García, F. Serna and J. L. de la Peña, *Polym. Rev.*, 2011, **51**, 341–390.
- 16 H. N. Kim, Z. Guo, W. Zhu, J. Yoon and H. Tian, *Chem. Soc. Rev.*, 2011, **40**, 79–93.
- 17 J. Hu, M. R. Whittaker, T. P. Davis and J. F. Quinn, *ACS Macro Lett.*, 2015, **4**, 236–241.
- 18 Z. Lin, Y. Ma, X. Zheng, L. Huang, E. Yang, C.-Y. Wu, T. J. Chow and Q. Ling, *Dyes Pigm.*, 2015, **113**, 129–137.
- 19 Y. Hu, Z. Zhao, X. Bai, X. Yuan, X. Zhang and T. Masuda, *RSC Adv.*, 2014, **4**, 55179.
- 20 F. Li, G. Wei, Y. Sheng, Y. Quan, Y. Cheng and C. Zhu, *Polymer*, 2014, **55**, 5689–5694.
- 21 F. Cheng, E. M. Bonder and F. Jakle, *J. Am. Chem. Soc.*, 2013, **135**, 17286–17289.
- 22 W. Y. Sung, M. H. Park, J. H. Park, M. Eo, M.-S. Yu, Y. Do and M. H. Lee, *Polymer*, 2012, **53**, 1857–1863.
- 23 W. Lu, D. Chen, H. Jiang, L. Jiang and Z. Shen, *J. Polym. Sci., Part A: Polym. Chem.*, 2012, **50**, 590–598.
- 24 Y. Jiang, X. Hu, J. Hu, H. Liu, H. Zhong and S. Liu, *Macromolecules*, 2011, **44**, 8780–8790.
- 25 B. G. Imsick, J. Raj Acharya and E. E. Nesterov, *Chem. Commun.*, 2013, **49**, 7043–7045.
- 26 I. H. A. Badr and M. E. Meyerhoff, *J. Am. Chem. Soc.*, 2005, **127**, 5318–5319.
- 27 E. Kim, H. Jung Kim, D. Ri Bae, S. Jin Lee, E. Jin Cho, M. Ryeong Seo, J. Seung Kim and J. Hwa Jung, *New J. Chem.*, 2008, **32**, 1003–1007.
- 28 H. Ma, B. S. Hsiao and B. Chu, *ACS Macro Lett.*, 2012, **1**, 213–216.
- 29 W. Luo, J. Schardt, C. Bommier, B. Wang, J. Razink, J. Simonsen and X. Ji, *J. Mater. Chem. A*, 2013, **1**, 10662.
- 30 N. Butchosa, C. Brown, P. T. Larsson, L. A. Berglund, V. Bulone and Q. Zhou, *Green Chem.*, 2013, **15**, 3404.
- 31 (a) Y. Habibi, *Chem. Soc. Rev.*, 2014, **43**, 1519–1542; (b) R. M. A. Domingues, M. E. Gomes and R. L. Reis, *Biomacromolecules*, 2014, **15**, 2327–2346.
- 32 F. Wang and D. Li, *Mater. Lett.*, 2015, **158**, 119–122.
- 33 K. Gao, Z. Shao, X. Wang, Y. Zhang, W. Wang and F. Wang, *RSC Adv.*, 2013, **3**, 15058.
- 34 M.-C. Li, Q. Wu, K. Song, S. Lee, Y. Qing and Y. Wu, *ACS Sustainable Chem. Eng.*, 2015, **3**(5), 821–832.
- 35 M.-C. Li, Q. Wu, K. Song, S. Lee, Y. Qing and Y. Wu, *ACS Appl. Mater. Interfaces*, 2015, **7**(8), 5006–5016.
- 36 W. Chen, Q. Li, Y. Wang, X. Yi, J. Zeng, H. Yu, Y. Liu and J. Li, *ChemSusChem*, 2014, **7**, 154–161.
- 37 L. Wang and M. Sanchez-Soto, *RSC Adv.*, 2015, **5**, 31384.
- 38 C. Wang, Y. Li, X. He, Y. Ding, Q. Peng and W. Zhao, *Nanoscale*, 2015, **7**, 7550.
- 39 X. Yao, W. Yu, X. Xu, F. Chen and Q. Fu, *Nanoscale*, 2015, **7**, 3959.
- 40 L. Melone, B. Rossi, N. Pastori, W. Panzeri, A. Mele and C. Punta, *ChemPlusChem*, 2015, **80**, 1408–1415.
- 41 V. Amendola, G. Bergamaschi, M. Boiocchi, L. Fabbriizzi and L. Mosca, *J. Am. Chem. Soc.*, 2013, **135**, 6345–6355.
- 42 V. Amendola, D. Esteban-Gómez, L. Fabbriizzi and M. Licchelli, *Acc. Chem. Res.*, 2006, **39**, 343–353.
- 43 D. Esteban-Gómez, L. Fabbriizzi and M. Licchelli, *J. Org. Chem.*, 2005, **70**, 5717–5720.
- 44 M. Boiocchi, L. Del Boca, D. Esteban Gómez, L. Fabbriizzi, M. Licchelli and E. Monzani, *J. Am. Chem. Soc.*, 2004, **126**, 16507–16514.
- 45 B. Kim, Y.-H. Kim, Y. Kim, J. Kang and W. Lee, *J. Mater. Chem. A*, 2014, **2**, 5682–5687.
- 46 X. Yong, W. Wan, M. Su, W. You, X. Lu, Y. Yan, J. Qu, R. Liu and T. Masudac, *Polym. Chem.*, 2013, **4**, 4126–4133.
- 47 M.-J. Sua, W. Wana, X. Yonga, X.-W. Lub, R.-Y. n. Liub and J.-Q. Qu, *Chin. J. Polym. Sci.*, 2013, **31**, 620–629.
- 48 R. Sakai, A. Nagai, Y. Tago, S. Sato, Y. Nishimura, T. Arai, T. Satoh and T. Kakuchi, *Macromolecules*, 2012, **45**, 4122–4127.





- 49 R. Sakai, S. Okade, E. B. Barasa, R. Kakuchi, M. Ziabka, S. Umeda, K. Tsuda, T. Satoh and T. Kakuchi, *Macromolecules*, 2010, **43**, 7406–7411.
- 50 N. Singh, N. Kaur, J. Dunn, R. Behan, R. C. Mulrooney and J. F. Callan, *Eur. Polym. J.*, 2009, **45**, 272–277.
- 51 R. Kakuchi, Y. Tago, R. Sakai, T. Satoh and T. Kakuchi, *Macromolecules*, 2009, **42**, 4430–4435.
- 52 A. von Harpe, H. Petersen, Y. Li and T. Kissel, *J. Controlled Release*, 2000, **69**, 309–322.
- 53 A. Isogai, T. Saito and H. Fukuzumi, *Nanoscale*, 2011, **3**, 71–85.
- 54 L. Melone, L. Altomare, I. Alfieri, A. Lorenzi, L. de Nardo and C. Punta, *J. Photochem. Photobiol., A*, 2013, **261**, 53–60.
- 55 H. Tian, W. Xiong, J. Wei, Y. Wang, X. Chen, X. Jing and Q. Zhu, *Biomaterials*, 2007, **28**, 2899–2907.
- 56 E. Vismara, L. Melone, G. Gastaldi, C. Cosentino and G. Torri, *J. Hazard. Mater.*, 2009, **170**, 798–808.
- 57 The reported  $K$  and  $m$  values correspond to an average over three titration experiments. The  $m$  values, lower but close to 1, are in line with the titration profiles which do not show sigmoidal behaviour, a characteristic of strong cooperativity. Attempts to fit the UV-vis titration data by a simple 1 : 1 binding isotherm gave unsatisfactory results. Given the dispersity of the polymeric material, these data should be considered only as qualitative in nature.
- 58 The colorimetric tests shown in Fig. 6 and 8 were performed at 55 °C in order to obtain the color change more quickly. It is apparent that the kinetic of deprotonation of the sensing units in **TOCNF2-bPEI-Sens** (10%) is not very fast at room temperature. However, in Fig. S15,† a comparison of the color change observed for the same material kept for 30 min at different temperatures is also shown. The colorimetric test was also performed in MeCN (see Fig. S16†) giving results qualitatively similar to those in DMSO.
- 59 X. Wu, X.-X. Chen, B.-N. Song, Y.-J. Huang, W.-J. Ouyang, Z. Li, T. D. James and Y.-B. Jiang, *Chem. Commun.*, 2014, **50**, 13987.
- 60 N. Kumari, N. Dey and S. Bhattacharya, *Analyst*, 2014, **139**, 2370.
- 61 M. Hirai and F. P. Gabbaï, *Chem. Sci.*, 2014, **5**, 1886.

